Pure Appl. Chem., Vol. 77, No. 6, pp. 1035–1050, 2005.
DOI: 10.1351/pac200577061035

Electronic energy transfer in dinuclear metal complexes containing *meta*-substituted phenylene units*

A. D'Aléo, S. Welter, E. Cecchetto, and L. De Cola‡

Universiteit van Amsterdam, HIMS, Nieuwe Achtergracht, 166, 1018 WV Amsterdam, The Netherlands

Abstract: The synthesis and photophysical properties of heterometallic dinuclear complexes based on ruthenium and osmium trisbipyridine units, Ru-*m*Ph_3-Os and Ru-*m*Ph_5-Os, in which the metal complexes are linked via an oligophenylene bridge centrally connected in the *meta* position, are described. Electronic energy transfer from the excited ruthenium-based component (donor) to the osmium moiety (acceptor) has been investigated using steady-state and time-resolved spectroscopy. The results obtained for the *meta*-substituted compounds are compared with the analogous systems in which the phenylene spacers are substituted in the *para* position. The mechanism of energy transfer is discussed.

Keywords: luminescence; ruthenium complexes; osmium complexes; energy transfer; conjugated systems.

INTRODUCTION

The investigation and understanding of energy-transfer processes in metal complex-based systems has received a lot of attention because of fundamental and applied implications [1–13]. A great effort has been devoted to the design and study of compounds able to collect electronic energy and funnel it to a single chromophore (antenna systems) in order to mimic natural photosynthetic species [14–19]. Besides the intrinsic absorption properties that the energy collectors must possess, a crucial aspect is the electronic interaction amongst the chromophores in order to have an efficient energy transfer. For systems in which the donor and acceptor pairs are covalently linked, through the so-called "bridging ligand", the structural and electronic properties of the connection play a major role [20–26]. The possibility of tuning the excited electronic-state interactions between the donor and acceptor components is related to the spectroscopic properties of the chromophores involved in the photoinduced processes. In a through-bond mechanism, the coupling is also strongly dependent on the properties of the bridging ligand [27–29]. Therefore, the structural and electronic features of the bridge are key factors for the energy- or charge-transfer processes. The desire to have long-range and vectorial photoinduced [30] processes has pushed the development of systems containing long-lived excited-state donor units, such as ruthenium polypyridine derivatives, and rigid, modular, conjugated connectors [31–33]. The acceptor unit must possess lower-lying excited states. Often, for energy-transfer processes, luminescent moieties such as osmium polypyridine complexes have been employed [34–36]. In many cases, the mechanism for the energy-transfer reaction is hard to assign because of the difficulties to construct systems

*Paper based on a presentation at the XXth IUPAC Symposium on Photochemistry, 17–22 July 2004, Granada, Spain. Other presentations are published in this issue, pp. 925–1085.

‡Corresponding author: E-mail: ldc@science.uva.nl

in which it is possible to vary only one parameter at the time, e.g., the distance between the donor acceptor moieties, geometry, or electronic nature of the bridging ligand, and the lack of easy calculation of the orbital overlap integral. Even in a Förster-type mechanism, in which it is possible to estimate the rate of the process by spectral data, the uncertainty related to the distance between the donor–acceptor units and the difficulties related to an accurate value of the orientation factor often prevent a final attribution of the mechanism.

It was also recently shown [37], for electron-transfer processes, that even in a through-bond interaction the use of "conducting" spacers could lead to a different mechanism for the photoinduced processes. Going from small bridging ligands to larger systems containing many spacer units, the energy of the lowest unoccupied molecular orbital (LUMO) is lowered and the electronic coupling between the acceptor and the donor is enhanced. Such an effect has been observed for systems containing polyphenylenevinylene units between a donor and an electron acceptor moiety [37]. By increasing the number of aromatic units, a switch from superexchange to hopping mechanism has been observed and a consequent reduction of the distance dependence on the rate of the process was reported.

When the bridging ligand consists of aromatic units, an interesting role is not only played by the number of spacers, but also by the position of substitution, in order to connect the donor and acceptor moieties. In fact, substitution in the *ortho*, *meta*, or *para* position on a phenyl ring could lead to different electronic coupling of the substituents as already demonstrated by Brédas for phenylenevinylene derivatives [38].

Here we report on the synthesis of heterometallic dinuclear ruthenium/osmium trisbipyridine complexes linked by oligophenylene units (3 or 5) as bridging ligand. In our systems, **Ru-*m*Ph$_3$-Os** and **Ru-*m*Ph$_5$-Os**, the central phenylene moiety is substituted in the *meta* position (Chart 1). The photophysical and electrochemical properties have been investigated, and electronic energy transfer from the excited ruthenium-based component to the osmium center is discussed. The role played by the *meta* connection, "loss in conjugation", is shown by comparing the novel complexes with the correspondent *para*-substituted compounds [39].

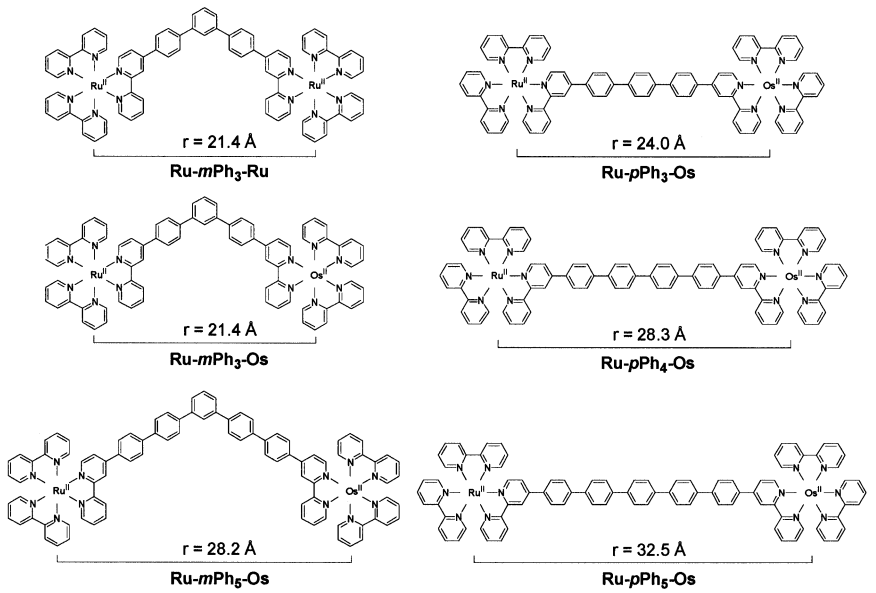

Chart 1 Schematic representation of the investigated complexes and their abbreviations. The correspondent *para* systems [39] and the metal–metal distances are also shown.

RESULTS AND DISCUSSION

All of the structures of the complexes prepared and investigated, their abbreviations, and the metal–metal distances (*r*) are depicted in Chart 1. For comparison, the analogous *para* oligophenylene compounds [39] are also shown. The homonuclear **Ru-*m*Ph$_3$-Ru** complex has been prepared and studied because it represents an excellent model compound for the heterometallic complexes. It is interesting to notice that the *meta* substitution results in a shortening of the metal–metal distance due to the bending of the complexes.

Synthesis

The homometallic compound **Ru-*m*Ph$_3$-Ru**, was synthesized from 1,3-phenylenebisboronic acid (**11**) and the ruthenium complex **1** in a one-step reaction (Scheme 1).

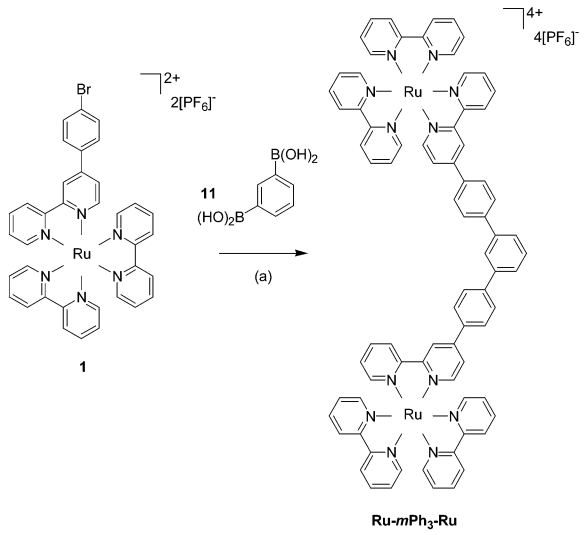

Scheme 1 Synthesis of the reference compound **Ru-*m*Ph$_3$-Ru**; (a) DMF, K_2CO_3, $Pd(PPh_3)_4$ T = 80 °C.

The preparation of the heterometallic complexes was carried out via a multi-step procedure [39]. Due to the low solubility of the polyphenylene units, the general procedure of preparing the free ligand was replaced by the so-called "chemistry on the complex" [40–43].

Using such an approach, the metal complexes (**3**, **7**, and **9**) were linked via Suzuki cross-coupling reactions [44,45] with phenylene units (**12** and **13**) in order to obtain the desired number of spacers (Scheme 2).

The last cross-coupling with the bipyridine boronic acid (**14**) [46] leads to the products **4** and **10** having a free chelating ligand to coordinate a second metal complex. This final complexation was performed in ethylene glycol with bpy_2OsCl_2 under microwave irradiation (2 × 2 min, 450 W) to yield **Ru-*m*Ph$_3$-Os** and **Ru-*m*Ph$_5$-Os**. All of the details of the synthesis and the characterization of the complexes are reported in the experimental section.

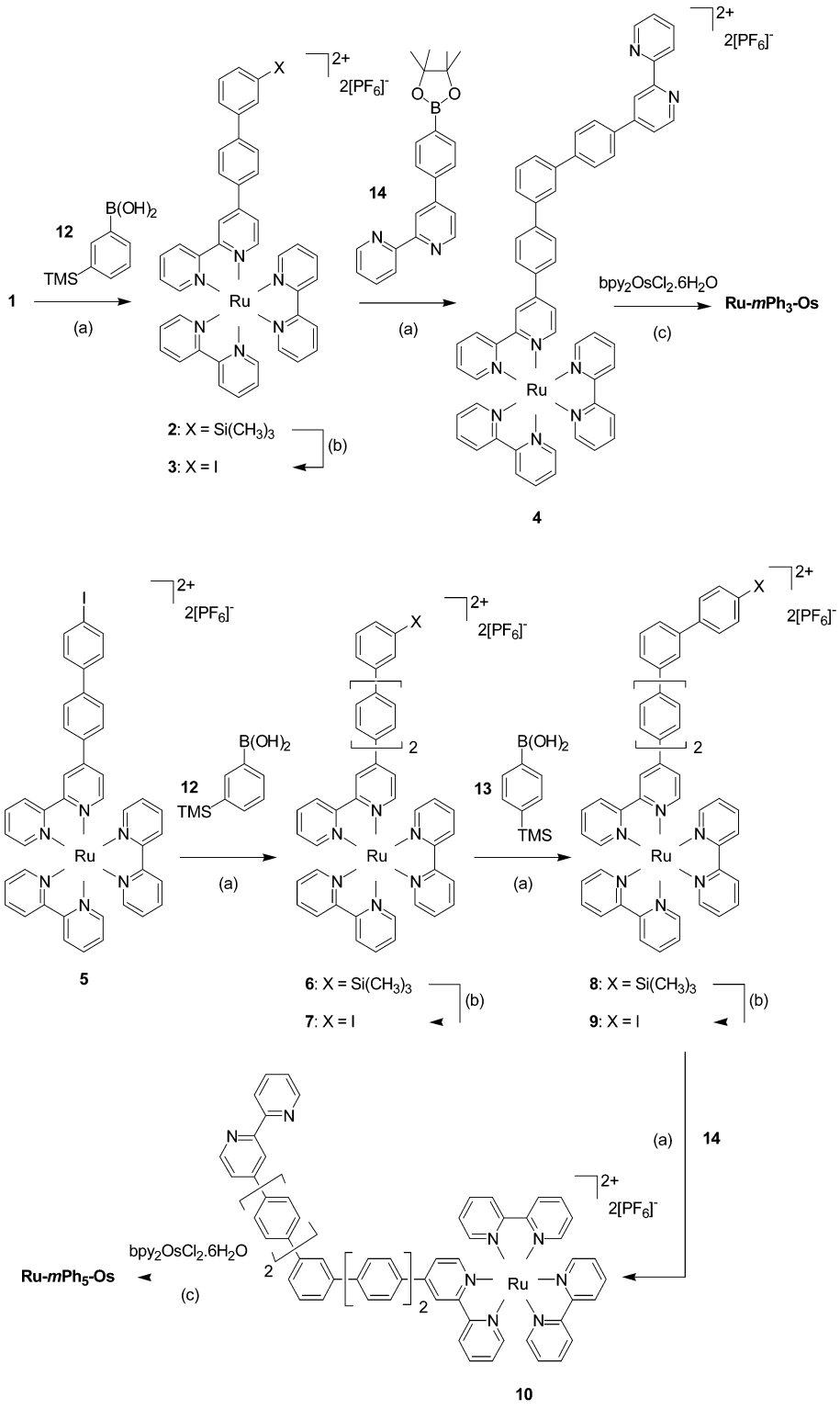

Scheme 2 Synthesis of **Ru-*m*Ph$_3$-Os** and **Ru-*m*Ph$_5$-Os**; (a) DMF, K_2CO_3, $Pd(PPh_3)_4$, 90 °C, (b) ICl, CH_2Cl_2, 0 °C, (c) ethylene glycol, microwave irradiation, 450 W.

Photophysical properties

All of the photophysical measurements were performed in aerated acetonitrile solution, and the most relevant data are reported in Table 1.

Table 1 Room-temperature absorption and emission data in acetonitrile solutions.

Complexes	Absorption	Luminescence 298 K				
	λ_{max} (nm) ($\varepsilon \times 10^3$ L mol^{-1} cm^{-1})	λ_{max} (Ru) (nm)	λ_{max} (Os) (nm)	τ (Ru) (ns)	τ (Os) (ns)	k_{en} ($\times 10^9$ s^{-1})
Ru-*m*Ph$_3$-Ru	290 (130), 326 (45), 455 (3.1)	626	–	205	–	–
Ru-*m*Ph$_3$-Os	290 (141), 325 (56), 455 (31), 600 (3)	630	753	0.780	43	1.3
Ru-*m*Ph$_5$-Os	290 (145), 333 (68), 455 (31), 600 (3)	629	752	14	43	0.067
Ru-*p*Ph$_2$-Os	290 (130), 324 (46), 457 (34), 600 (3)	–	752	0.004	43	249
Ru-*p*Ph$_3$-Os	290 (131), 342 (54), 457 (34), 600 (3)	620	751	0.017	43	59
Ru-*p*Ph$_4$-Os	290 (126), 345 (57), 456 (31), 600 (2.9)	617	753	0.245	43	4.1
Ru-*p*Ph$_5$-Os	290 (138), 347 (74), 457 (34), 600 (3.1)	621	751	2.020	43	0.49

UV/vis absorption spectroscopy

The UV/vis absorption spectra of the *meta* and *para* complexes are displayed in Fig. 1. The spectra show intense absorption bands at 290 nm attributed to the π-π* transitions involving the bipyridine ligands coordinated to the metal ions. Also in the UV region (between 320 and 350 nm), intense bands are observed due to the π-π* transitions of the phenylene spacers. As expected, these bands shift to lower energy upon increasing the number of phenyls. In fact, the conjugation increases with the number of units until the effective conjugation length is reached [47]. The absorption spectra of the *para* metal complexes show a very minor red-shift going from four to five phenylenes. This indicates that the effective conjugation length is already almost reached with five spacer units [39,48]. It is interesting to note that the 320–350-nm bands for the *meta* complexes are blue-shifted compared to the *para* analogs. This effect is again related to the conjugation of the phenylene bridge. It is known that for *meta* substitution the electronic coupling between adjacent phenyls is lower than for the correspondent *para* systems [38]. Observing the structure of the *meta*-substituted complexes (Chart 1), one can imagine that the complexes with three **Ru-*m*Ph$_3$-Os** and five **Ru-*m*Ph$_5$-Os** phenylenes are constituted by two "isolated" metal trisbipyridine parts each substituted with two and three phenylene units, respectively. Therefore, the absorption due to the π-π* transitions located on the phenylenes, assuming that the *meta*-substituted phenyl acts as an insulator, should mirror this effect and a biphenyl-type absorption should be expected. The absorption maxima of the phenylene units for **Ru-*m*Ph$_3$-Os** and **Ru-*m*Ph$_5$-Os** are 325 and 333 nm, respectively, while for **Ru-*p*Ph$_2$-Os**, **Ru-*p*Ph$_3$-Os**, and **Ru-*p*Ph$_5$-Os** they are 324, 342, and 347 nm, respectively. Therefore, the *meta* complexes (**Ru-*m*Ph$_3$-Os** and **Ru-*m*Ph$_5$-Os**) are more similar to the corresponding *para* complexes containing only two and three phenylene spacers, respectively (**Ru-*p*Ph$_2$-Os** and **Ru-*p*Ph$_3$-Os**). The insulating effect of the *meta* substitution was already described for other conjugated systems by Brédas et al. [38] and very recently for dinuclear complexes by Vos et al. [26].

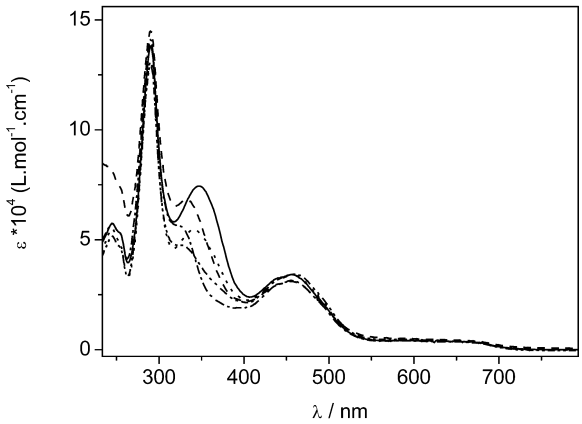

Fig. 1 UV/vis absorption spectra of **Ru-*p*Ph$_2$-Os** (–··–), **Ru-*m*Ph$_3$-Os** (–·–), **Ru-*p*Ph$_3$-Os** (···), **Ru-*m*Ph$_5$-Os**, **(---)** and **Ru-*p*Ph$_5$-Os** (—) recorded in acetonitrile solutions.

In the visible region, the ^{1}MLCT bands of the ruthenium and of the osmium moieties are observed. The ruthenium band is centered at 450 nm, while the transitions for the osmium-based component fall at lower energy, at about 480 nm (Fig. 1). As for any osmium trisbipyridine compound, a weaker broad band around 600 nm ($\varepsilon = 3000$ L mol^{-1} cm^{-1}) is observed. Such absorption is due to spin-forbidden transitions from the ground to the lowest ^{3}MLCT excited states. Because osmium is a heavy metal, these transitions are partially allowed due to the strong spin-orbital coupling [34]. The MLCT transitions are not affected by *meta* vs. *para* substitutions since, in any case, the electronic coupling between the terminal metal units is very weak. This is also confirmed by comparing the absorption spectra of the mononuclear species **Ru-Ph$_2$** and **Os-Ph$_2$** with the heterometallic **Ru-*m*Ph$_3$-Os** complex. In Fig. 2, a comparison of the species shows that an isosbestic point is present at about 440 nm, which will be used as excitation wavelength since 50 % of the light is absorbed by the ruthenium moiety and 50 % by the osmium moiety in the **Ru-*m*Ph$_3$-Os** (——) complex.

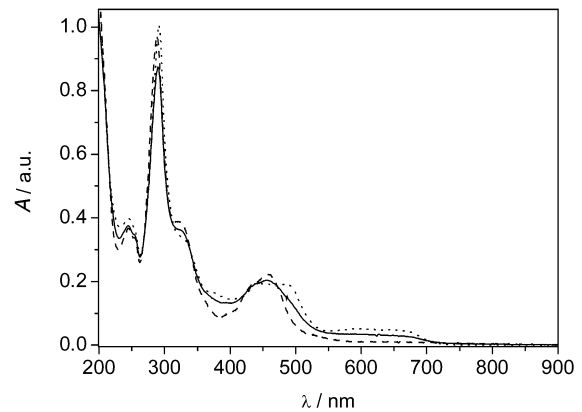

Fig. 2 UV/vis absorption spectra in acetonitrile solution showing the isosbestic point at about 440 nm for monomeric ruthenium (**---**), monomeric osmium (···), and the heterometallic **Ru-*m*Ph$_3$-Os** (—) complexes. Please note that for the monomeric species, the spectra have been multiplied by 2.

Steady-state luminescence

All of the compounds investigated show two broad structureless emissions centered at about 630 nm and at 750 nm from the two metal-based units (Fig. 3). The high-energy emission band is due to the ruthenium-based component, while the lower-energy band is attributed to the osmium-based ^{3}MLCT emission. By comparison with the homometallic compound (**Ru-*m*Ph$_3$-Ru**), it can be easily seen that the ruthenium-centered emission in the heterometallic compounds is strongly quenched (more than 10 times for **Ru-*m*Ph$_5$-Os** and more than 100 times for **Ru-*m*Ph$_3$-Os**). Such a quenching is accompanied by a sensitization of the osmium emission that has the same emission quantum yield as the homometallic **Os-*p*Ph$_n$-Os** ($\phi = 4.2 \times 10^{-3}$) [46]. This spectroscopic behavior can be easily interpreted as an efficient energy transfer from the excited ruthenium-based component (donor) to the lowest excited state located on the osmium moiety (acceptor). In order to have a quantitative analysis of the process, the emission spectra were recorded by exciting at 440 nm, where 50 % of the light excites the ruthenium component and 50 % is absorbed by the osmium unit (see Fig. 2). The residual ruthenium emission from the longest dinuclear compound has a much higher quantum yield than the shorter molecule. This is in good agreement with different distances between the donor–acceptor pair (21.4 Å for **Ru-*m*Ph$_3$-Os** and 28.2 Å for **Ru-*m*Ph$_5$-Os**, see Chart 1). By increasing the distance between the two metal centers, the electronic coupling decreases and the energy transfer is slowed down. However, as will be discussed in the next section, since a through-bond superexchange mechanism is responsible for the energy-transfer process, the *meta* vs. *para* position on the substitution of the phenylene units plays the most important role in reducing the electronic coupling between the metal units.

In order to evaluate the rates of the energy-transfer process, time-resolved emission and transient absorption spectroscopy were performed on the complexes.

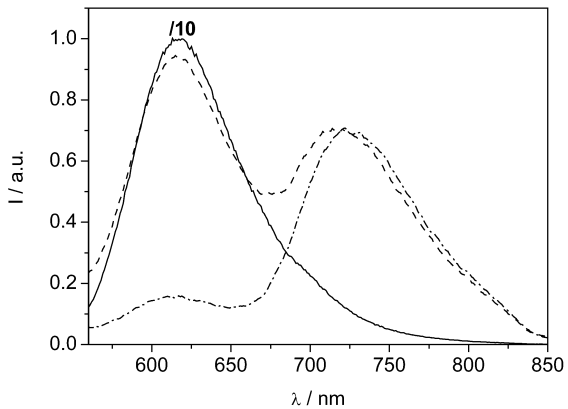

Fig. 3 Room-temperature emission spectra of **Ru-*m*Ph$_3$-Ru** (—) (divided by 10), **Ru-*m*Ph$_3$-Os** (–·–), and **Ru-*m*Ph$_5$-Os** (---) in acetonitrile solutions. All of the compounds have the same absorbance at the excitation wavelength (λ_{ex} = 440 nm).

Time-resolved spectroscopy

The luminescent excited-state lifetimes of all the complexes were determined by single photon counting or streak camera techniques, and the results are summarized in Table 1. For **Ru-*m*Ph$_5$-Os**, the ruthenium-based component, monitored at 600 nm, has a much shorter excited-state lifetime (τ = 14 ns) than the reference dinuclear complex, **Ru-*m*Ph$_3$-Ru** (τ = 205 ns). Such fast decay of the luminescent state is in good agreement with the emission quantum yield of the ruthenium moiety, which is 12 times lower than the quantum yield of the homometallic compound. For the **Ru-*m*Ph$_3$-Os** complex, the excited-state lifetime of the ruthenium component (τ = 780 ps) is even shorter than for the **Ru-*m*Ph$_5$-Os** com-

plex. The luminescent excited state of the ruthenium component is quenched by the low-lying excited state of the osmium component (see Fig. 4a) that for the **Ru-*m*Ph$_3$-Os** is populated with a time constant, risetime, of 700 ps (Fig. 4b). The excited osmium unit then decays within 43 ns to the ground state in both complexes (the same excited-state lifetime was also found for *para*-substituted complexes) [46]. The energy-transfer process for both complexes is thermodynamically allowed (ΔG = –0.38 eV, see Fig. 4a). As expected, the rate of the energy transfer depends on the distance between the two chromophores. The rate is about 20 times faster for the shorter complex **Ru-*m*Ph$_3$-Os** than for **Ru-*m*Ph$_5$-Os** (see Table 1).

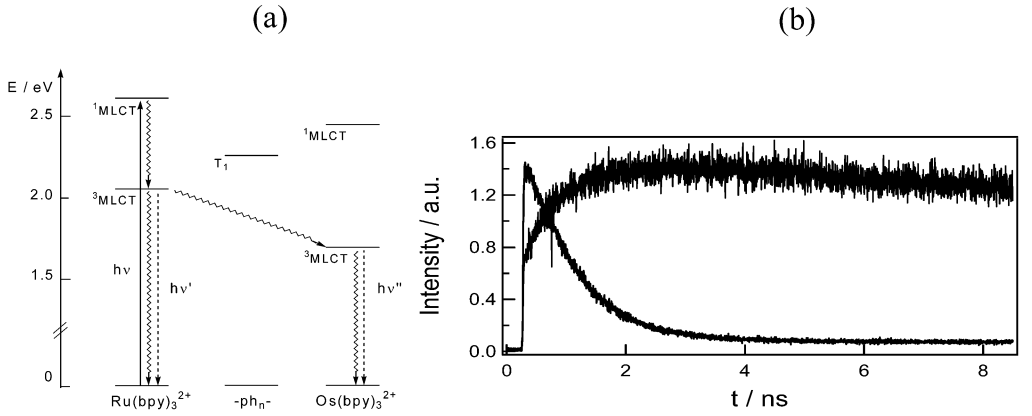

Fig. 4 (a): Simplified energy scheme of the states involved in the processes. (b): Decay of the ruthenium-based component (780 ps) and risetime (700 ps) monitored on the osmium-based component, for **Ru-*m*Ph$_3$-Os** in air-equilibrated acetonitrile (λ_{ex} = 324 nm).

A comparison with the *para*-substituted complexes **Ru-*p*Ph$_3$-Os** and **Ru-*p*Ph$_5$-Os** reveals that the photoinduced processes are, at least, one order of magnitude slower for the *meta* complexes. Such behavior already suggests that a Förster-type energy-transfer mechanism can be ruled out. The spectral overlap for the ruthenium-osmium pair is reasonably good, and of course is the same for both series of complexes since the absorption of the acceptor and the emission properties of the donor are not affected by the substitution position of the phenylene spacer. On the other hand, the distance between the donor and acceptor pairs in the case of the *meta* complexes is smaller than the correspondent *para* compounds due to the bending of the bridging ligand (see Chart 1). Therefore, for a pure Förster energy-transfer process, on the basis of distance and spectral overlap integral, the rates of the *meta* complexes should be faster than for the linear *para* analogs.

The energy-transfer rate via a Förster-type mechanism can in fact be calculated using eq. 1:

$$k_{en} = 1/\tau^\circ \ (R_0/r)^6 \tag{1}$$

where τ° is the decay time of the donor without acceptor, R_0 is the critical Förster radius, and r is the donor-to-acceptor distance [49] (see Chart 1).

To calculate the Förster distance R_0, the simplified eq. 2 can be applied:

$$R_0^6 = (8.8 \times 10^{-25}\ K^2 \Phi J_F)/(n^4 \tau^\circ k_{en}) \qquad \text{with } J_F = \int F(\nu)\nu(\nu)\nu^{-4} d\nu \tag{2}$$

where n is the refractive index of the medium, Φ° is the quantum yield of the donor in the absence of the acceptor, and J_F is the overlap integral of the donor emission and the acceptor absorption.

From the experimental spectroscopic data, R_0 was estimated to be about 36 Å in our systems. In such a case, the energy-transfer rate, calculated by the Förster-type mechanism, can be estimated to be 1.2×10^8 s^{-1} and 2.4×10^7 s^{-1} for **Ru-*m*Ph$_3$-Os** and **Ru-*m*Ph$_5$-Os**, respectively.

The experimental values obtained for the *meta* systems (see Table 1) are very different from the calculated ones (1.3×10^9 s^{-1} for **Ru-*m*Ph$_3$-Os** and 6.7×10^7 s^{-1} for **Ru-*m*Ph$_5$-Os**). Such discrepancies for the energy-transfer rates could be explained by the large uncertainty in the estimation of the metal-to-metal distance in metal complexes in which the lowest excited state is an MLCT involving the bridging ligand. In fact, upon excitation of the donor moiety, the exciton is not localized on the bipyridine, but it extends to the phenylene units present as substituents on one of the bipyridine (see also next section of the transient absorption spectroscopy). Therefore, the distance calculated using simple molecular modeling does not reflect the real situation in systems in which delocalization plays a major role. Nevertheless, the same argument applies for the *para*-substituted compounds, and it can be easily seen that the distance between the two metal centers is much smaller in the *meta*-substituted complexes (21.4 Å for **Ru-*m*Ph$_3$-Os** vs. 24.0 Å for **Ru-*p*Ph$_3$-Os**, and 28.2 Å for **Ru-*m*Ph$_5$-Os** vs. 32.5 Å for **Ru-*p*Ph$_5$-Os**) (see Chart 1). Thus, since the lowest excited state is the same for both families of complexes, it is clear that the electronic factors related to the substitution on the phenylene rings must play a major role by influencing the electronic coupling between the two chromophores and, therefore, the orbital overlap, which is important for the Dexter mechanism [49]. A closer analysis of the excited-state levels of the bridging ligands suggests that the energy of such states is too high to mix with the donor or acceptor levels. Their direct involvement in the energy-transfer process can only be expected in a superexchange mechanism. In such a regime, the attenuation factor β can be calculated knowing the distance between the two metal units ($r = r' - r_0$, see ref. [50]) and the rates for the processes (k_{en}) using eq. 4 derived from eq. 3:

$$k_{en} = k_{en}(0)\exp[\beta(r' - r_0)] \tag{3}$$

$$\ln(k_{en}) = -\beta\, r + c, \text{ where } c \text{ is a constant} \tag{4}$$

Plotting the logarithm of k_{en} vs. the distance leads to a β value of 0.44 $Å^{-1}$ (Fig. 5). This value is in excellent agreement with the β value obtained for polyphenylene units and for the *para* complexes (0.50 $Å^{-1}$) (Fig. 5). It is also interesting to notice that the rates decrease exponentially with increasing distance, as expected in a superexchange regime [51–53].

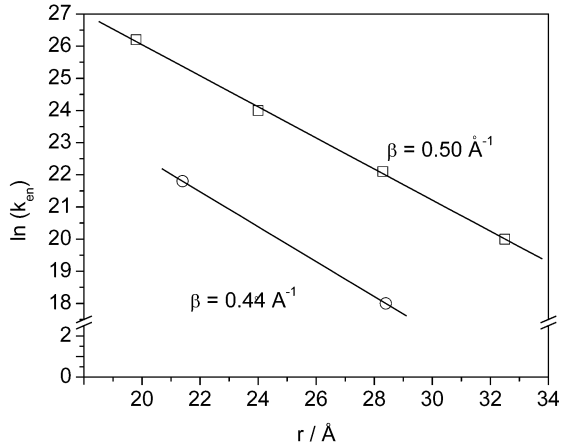

Fig. 5 Logarithm of the energy-transfer rate vs. donor–acceptor distance (□: *para*-substituted complexes, ○: *meta*-substituted complexes). Attenuation factors β are evaluated by linear fit.

In previously reported dinuclear systems containing a *meta*-substituted phenylene bridging ligand, the energy-transfer processes were attributed to a Förster-type mechanism [26]. In fact, for such systems. the lowest excited state involved the peripheral bipyridine since the chelating site residing on the bridging ligand was an electron reach moiety.

A further confirmation of the energy-transfer process and of the involvement of the bridging ligand in the photoinduced excitation was obtained by subpicosecond absorption transient absorption spectroscopy (Fig. 6).

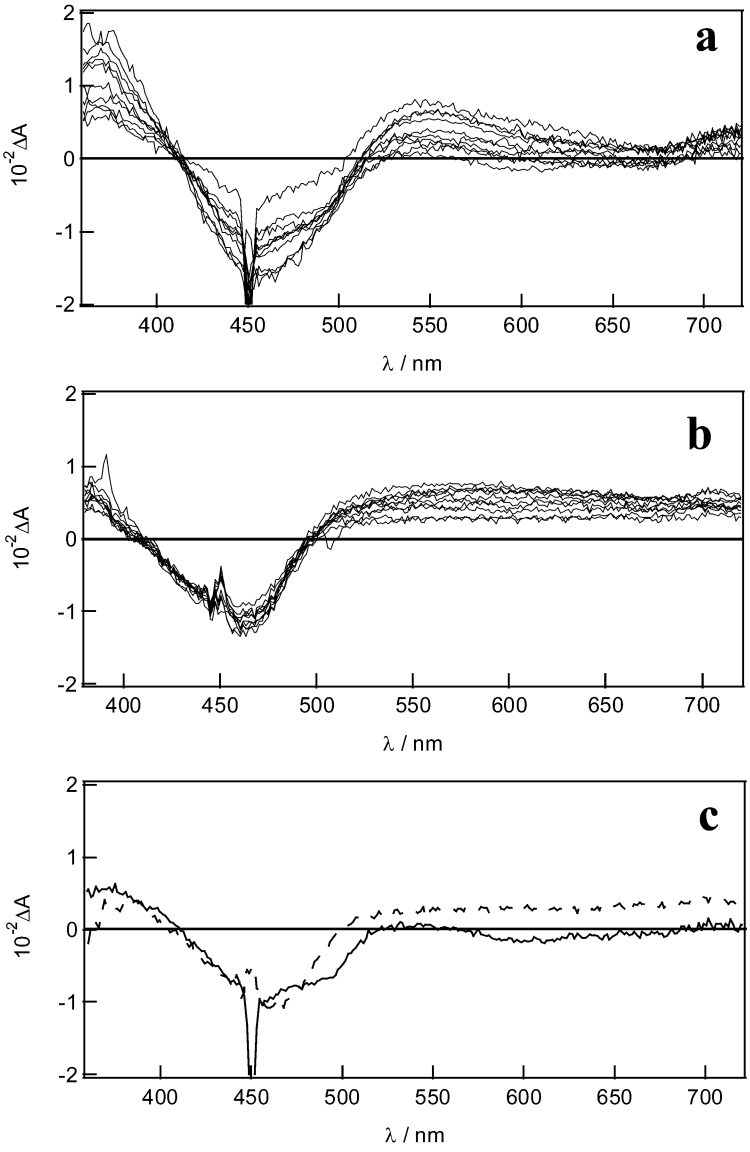

Fig. 6 Subpicosecond transient absorption spectra of (a) **Ru-*m*Ph$_3$-Os** and (b) **Ru-*m*Ph$_3$-Ru**, recorded in air-saturated acetonitrile at room temperature (λ_{ex} = 450 nm). The increment between each frame is 100 ps. Subpicosecond transient absorption spectra of **Ru-*m*Ph$_3$-Os** (—) and **Ru-*m*Ph$_3$-Ru** (---) 800 ps after the laser pulse (λ_{ex} = 450 nm) are shown in c.

For the model complex, **Ru-*m*Ph$_3$-Ru**, in which no energy transfer is possible, upon light excitation (λ_{exc} = 450 nm) the MLCT state is formed, resulting in the formation of the radical anion of the bipyridine, visible at about 370 nm and of the bleaching in the visible region 420–480 nm (Fig. 6b). A

broad absorption band is also observed in the visible region of the spectrum attributed to the partial delocalization of the charge on the phenylene units attached to the bridging bipyridine ligand [46].

Interestingly, a differential spectrum obtained by superimposition of the spectra of the **Ru-*p*Ph$_3$-Ru** and **Ru-*m*Ph$_3$-Ru** under identical experimental conditions shows that, for the *meta*-substituted complex, the visible band is less intense. Even more interestingly, the bipyridine radical anion band is blue-shifted by about 10 nm (centered at 370 and 380 nm for **Ru-*m*Ph$_3$-Ru** and **Ru-*p*Ph$_3$-Ru**, respectively) as expected for less conjugated systems.

The transient spectrum for the **Ru-*m*Ph$_3$-Os** complex shows more intriguing features (Fig. 6a). In fact, the bleaching due to the formation of the excited state of the ruthenium evolves over time, forming a new band at very close energy. Furthermore, the broad absorption between 550 and 700 nm is now less pronounced, and a clear bleaching in the 600–700 nm region is observed. In order to identify better such small spectral changes, we have performed the same measurement on isoabsorptive solutions of the homometallic **Ru-*m*Ph$_3$-Ru** and the heterometallic **Ru-*m*Ph$_3$-Os** compounds under identical experimental conditions (Fig. 6c). The spectra shown in Fig. 6c were recorded after 800 ps, and they clearly show that the MLCT bleaching band due to the ruthenium moiety excitation in the mixed metal complex has a broader and distinguishable feature at 490 nm. From the absorption spectrum (Fig. 1), a strong overlap of the ruthenium-based component and the osmium transitions between 430 and 490 nm are observed, which prevents a full separation of the two bands. The formation of the osmium excited state can also be evidenced by the bleaching at about 600 nm due to the spin-forbidden MLCT band (see also absorption spectrum, Fig. 1). The kinetics for the disappearance of the ruthenium excited state (880 ps) and formation of the osmium luminescent state (800 ps) are in good agreement with what was measured by emission spectroscopy. Therefore, we can conclude that a fast energy transfer (1.3×10^9 s^{-1}) is observed for the complexes (**Ru-*m*Ph$_n$-Os**). However, this energy transfer depends on the phenylene substitution as shown by the faster energy-transfer rate for the *para* complexes (60 times faster than for the *meta*).

CONCLUSION

We have prepared and characterized two new heterometallic complexes containing ruthenium and osmium trisbipyridyl moieties connected by an oligophenylene bridge with a central *meta*-substituted unit. Their photophysical properties have been investigated using steady-state and time-resolved spectroscopy. We have shown that energy transfer takes place from the excited ruthenium-based component to the lowest excited state localized on the osmium unit. The rates of the photoinduced processes strongly depend on the distance between the two chromophores. By comparison with the *para*-substituted analog complexes, it has been demonstrated that the bridging ligand plays a key role. In particular, due to the *meta* substitution, the electronic coupling between the energy donor and acceptor moieties decreases. Therefore, slower energy-transfer processes have been observed, compared with the *para*-substituted complexes, even though the metal–metal distance between the ruthenium and osmium components is smaller for the *meta* than for the *para* compounds. On the basis of these results and by comparison between the Förster calculated rates and the experimental findings, we have attributed the energy transfer to a superexchange mechanism. We believe that our results are of interest not only for a full understanding of the role played by key factors such as distance, nature, and geometry of the bridging ligands, but also for the design of systems in which a partial and tunable energy-transfer process could lead to interesting effects such as white light generation from blue and red metal complexes [54].

EXPERIMENTAL

All chemicals were purchased from Acros or Aldrich and were used as received. All solvents for the synthesis were purchased and used in analytic grade. For the spectroscopy, spectroscopic grade solvents

were used. Compounds **1**, **5** [55], and **14** [39] were synthesized according to literature procedures. All purification by chromatography was performed with a water, methanol, acetonitrile, and NaCl mixture (1:4:1:0.1 %) (magic mixture). ^{1}H NMR spectra were obtained with a Varian Gemini-300 spectrometer. Chemical shifts (δ) are given in ppm, using the residual nondeuterated solvent as internal standard.

The UV/vis absorption spectra were recorded on a Hewlett Packard diode array 8453 spectrophotometer. Recording of the emission spectra was done with a SPEX 1681 Fluorolog spectrofluorometer. Low-temperature emission spectra were recorded in 5-mm-diameter quartz tubes that were placed in a Dewar filled with liquid nitrogen and equipped with quartz walls. The emission spectra were corrected for monochromator and photomultiplier efficiencies and for the xenon lamp stability. Lifetimes were determined using a Coherent Infinity Nd:YAG-XPO laser (1 ns pulses FWHM) and a Hamamatsu C5680-21 streak camera equipped with a Hamamatsu M5677 low-speed single-sweep unit.

A subnanosecond single-photon counting set-up was used for time-resolved fluorescence measurements. The excitation source consists of a frequency-doubled (300–340 nm, 1 ps, 3.8 MHz) output of a cavity dumped DCM dye laser (Coherent model 700) that was pumped by a mode-locked Ar-ion laser (Coherent 486 AS Mode Locker, Coherent Innova 200 laser). A micro channel plate photomultiplier (Hamamatsu R3809) was used as detector.

Subpicosecond transient absorption spectroscopy experiments were performed on a Spectra-Physics Hurricane Titanium:Sapphire regenerative amplifier system. The optical bench assembly of the Hurricane includes a seeding laser (Mai Tai), a pulse stretcher, a Titanium:Sapphire regenerative amplifier, a Q-switched pump laser (Evolution) and a pulse compressor. The 800-nm output of the laser is typically 1 mJ/pulse (130 fs) at a repetition rate of 1 kHz. A full-spectrum set-up based on an optical Parametric amplifier (Spectr-Physics OPA 800) as pump and residual fundamental light (150 μJ/pulse) from the pump OPA was used for white light generation, which was detected with a CCD spectrometer. The white light generation was accomplished by focusing the fundamental (800 nm) into a H_2O flow-through cell (10 mm).

Synthesis of Ru-*m*Ph_3-Ru

In a 100-ml Schlenk flask, **1** (50 mg, 0.048 mmol), **11** (4 mg, 0.024 mmol), and K_2CO_3 (40 mg, 0.290 mmol) were mixed in DMF (15 ml) and the solution was degassed. To the solution, $Pd(PPh_3)_4$ (6 mg, 0.005 mmol) was added. The reaction was stirred at 80 °C under nitrogen during 16 h. The DMF was removed under vacuum, and the solid was purified by column chromatography (silica gel) using magic mixture as eluant. The organic solvents were evaporated, and the complex was precipitated from water by adding NH_4PF_6 (50 mg). The precipitate was filtered, washed with water and diethyl ether, and extracted using acetonitrile. The solvent was evaporated, and the orange solid was dried at 80 °C overnight under vacuum. Yield: 50 % (M = 1945.12 g mol^{-1}); ^{1}H NMR (CD_3CN): δ = 8.83 (m, 2H), 8.74 (m, 2H), 8.59–8.47 (m, 8H), 8.18–7.95 (m, 21H,), 7.94–7.66 (m, 15H), 7.50–7.42 (m, 5H), 7.40–7.30 (m, 5H).

General procedure for the synthesis of complexes 2, 6, and 8

In a 100-ml Schlenk flask, complex-PhX (X = Br or I) (**1**, **5**, **7**) (1 equiv), 1-trimethylsilylphenylboronic acid (**12** or **13**) (1.3 equiv) and K_2CO_3 (7 equiv) were mixed in DMF (10–15 ml) and the solution was degassed. A catalytic amount of $Pd(PPh_3)_4$ was added (0.1 equiv). The reaction was heated overnight at 90 °C under nitrogen. The DMF was removed under vacuum. The solid was purified by column chromatography (silica gel) using magic mixture as eluant. Finally, the orange solid was dried at 80 °C overnight under vacuum.

2. Yield: 87 % (M = 1160.06 g mol^{-1}); ^{1}H NMR (CD_3CN): δ = 8.82 (m, 1H), 8.75–8.72 (d, ^3J = 8.4 Hz, 1H), 8.56–8.52 (m, 4H), 8.13–8.06 (m, 5H), 8.01–7.98 (d, 2H), 7.98–7.95 (d, ^3J = 8.1 Hz, 2H),

7.90–7.81 (d, 4H), 7.80–7.76 (m, 6H), 7.70–7.64 (m, 1H), 7.63–7.59 (d, ^3J = 7.5 Hz, 1H), 7.53–7.47 (t, ^3J = 7.5 Hz, 1H), 7.46–7.40 (m, 6H), 0.33 (s, 9H).

6. Yield: 68 % (M = 1083.94 g mol^{-1}); ^{1}H NMR (CD_3CN): δ = 8.82 (m, 1H), 8.75–8.72 (d, ^3J = 7.5 Hz, 1H), 8.57–8.52 (m, 4H), 8.15–8.06 (m, 5H), 8.03–8.00 (d, ^3J = 8.1 Hz, 2H), 7.93–7.88 (m, 3H), 7.87–7.68 (d, ^3J = 6.4 Hz, 8H), 7.65–7.63 (dd, ^3J = 7.5 Hz, ^4J = 1.5 Hz, 1H), 7.55–7.52 (d, ^3J = 7.5 Hz, 1H), 7.47–7.40 (m, 5H), 0.34 (s, 9H).

8. Yield: 90 % (M = 1236.14 g mol^{-1}); ^{1}H NMR (CD_3CN): δ = 8.83 (m, 1H), 8.76–8.70 (d, ^3J = 8.1 Hz, 1H), 8.58–8.53 (m, 4H), 8.16–8.04 (m, 5H), 8.04–8.02 (d, ^3J = 8.7 Hz, 2H), 8.00–7.98 (m, 1H), 7.97–7.95 (d, ^3J = 8.4 Hz, 2H), 7.90 (m, 4H), 7.85–7.68 (m, 13H), 7.63–7.60 (d, ^3J = 7.5 Hz, 1H), 7.47–7.40 (m, 5H), 0.33 (s, 9H).

General procedure for the conversion of the trimethylsilyl group into iodo (derivatives 3, 7, and 9)

In a 100-ml round-bottom flask, **2**, **6**, or **8** (1 equiv) was solubilized in CH_2Cl_2 (45 ml) and the solution was cooled to 0 °C. Iodine chloride (4 equiv) in CH_2Cl_2 (5 ml) was then added slowly. The reaction was stirred for 1.5 h at 0 °C, then 2.5 h at room temperature. The reaction was quenched with a 1 M solution of $Na_2S_2O_5$ in water (50 ml). The organic phase was washed with water, and the solvent was removed under vacuum. The complex was solubilized in magic mixture, the volume of solvent reduced and the complex was precipitated by adding NH_4PF_6 (50 mg). The orange solid was dried for 3 h under vacuum at 60 °C.

3. Yield: 96 % (M = 1137.65 g mol^{-1}); ^{1}H NMR (CD_3CN): δ = 8.81 (m, 1H), 8.75–8.70 (d, ^3J = 7.8 Hz, 1H), 8.57–8.51 (m, 4H), 8.16–8.04 (m, 6H), 8.02–7.99 (d, ^3J = 8.1 Hz, 2H), 7.89–7.86 (d, ^3J = 7.8 Hz, 2H), 7.85–7.70 (m, 9H), 7.52–7.40 (m, 5H), 7.56–7.33 (d, ^3J = 7.8 Hz, 1H).

7. Yield: 88 % (M = 1213.77 g mol^{-1}); ^{1}H NMR (CD_3CN): δ = 8.83 (m, 1H), 8.76–8.70 (d, ^3J = 8.4 Hz, 1H), 8.58–8.53 (m, 4H), 8.16–8.05 (m, 5H), 8.04–8.02 (d, ^3J = 8.7 Hz, 2H), 7.98–7.95 (d, ^3J = 8.4 Hz, 2H), 7.90–7.70 (m, 12H), 7.47–7.40 (m, 8H), 0.33 (s, 9H).

9. Yield: 96 % (M = 1289.85 g mol^{-1}); ^{1}H NMR (CD_3CN): δ = 8.83 (m, 1H), 8.76–8.70 (d, ^3J = 8.1 Hz, 1H), 8.58–8.53 (m, 4H), 8.16–8.06 (m, 5H), 8.04–8.02 (d, 2H), 8.00–7.94 (m, 3H), 7.92–7.90 (m, 4H), 7.88–7.85 (m, 2H), 7.84–7.72 (m, 8H), 7.70–7.54 (m, 4H), 7.47–7.40 (m, 5H).

Synthesis of 4 and 10

In a 100-ml Schlenk flask, **3** or **9** (1 equiv), **14** (1.4 equiv) and K_2CO_3 (7 equiv) were mixed in DMF (10–15 ml), and the solution was degassed. A catalytic amount of $Pd(PPh_3)_4$ was added (0.1 equiv), and the reaction was stirred at 90 °C under nitrogen. The DMF was removed under vacuum. The solid was purified by column chromatography (silica gel) using magic mixture as eluant. Finally, the orange solid was dried at 80 °C overnight under vacuum.

4. Yield: 73 % (M = 1242.03 g mol^{-1}); ^{1}H NMR (CD_3CN): δ = 8.81 (m, 1H), 8.80–8.70 (m, 4H), 8.59–8.47 (m, 5H), 8.18–8.06 (m, 5H), 8.04–7.89 (m, 9H), 7.87–7.70 (m, 10H), 7.69–7.61 (m, 2H), 7.50–7.41 (m, 6H).

10. Yield: 78 % (M = 1394.23 g mol^{-1}); ^{1}H NMR (CD_3CN): δ = 8.83 (m, 1H), 8.80–8.70 (m, 4H), 8.59–8.47 (m, 5H), 8.18–8.06 (m, 5H), 8.04–7.86 (m, 19H), 7.82–7.69 (m, 8H), 7.68–7.61 (m, 2H), 7.50–7.41 (m, 6H).

General way for the preparation of bimetallic Ru-*m*Ph$_n$-Os complexes

$Bpy_2OsCl_2.6H_2O$ (1 equiv) and **4** or **10** (1 equiv), in ethylene glycol (5 ml), were homogenized in an ultrasonic bath. Subsequently, the solution was irradiated at 450 W for 2 min in a modified microwave

oven and, after a cooling down period, for another 2 min. After evaporating most of the ethylene glycol under vacuum, the complex was solubilized in water then NH_4PF_6 (50 mg) was added to precipitate the complex. The green precipitate formed was filtered, then reextracted with acetonitrile. The compound was purified by column chromatography (silica gel) using magic mixture as eluant. The solution was concentrated under vacuum. Then, the product was precipitated by adding NH_4PF_6 (50 mg) to the aqueous solution. The precipitate was filtered over Celite, washed with water and diethylether and reextracted with acetonitrile. The dark-green product was dried at 80 °C under vacuum overnight.

Ru-*m*Ph$_3$-Os. Yield: 29 % (M = 2034.53 g mol^{-1}); MS (ESI, m/z): 873.15 (M^+ –PF_6), 532.77 (M^+ – 2PF_6), 369.59 ($M^{+\cdot}$– 3PF_6); ^{1}H NMR (CD_3CN): δ = 8.83 (m, 2H), 8.74 (m, 2H), 8.59–8.47 (m, 8H), 8.18–8.01 (m, 14H), 7.99–7.94 (m, 4H), 7.92–7.66 (m, 18H), 7.50–7.40 (m, 5H), 7.41–7.30 (m, 5H).

Ru-*m*Ph$_5$-Os. Yield: 61 % (M = 2186.73 g mol^{-1}); MS (ESI, m/z): 948.67 (M^+ –PF_6), 583.79 (M^+ – 2PF_6), 401.85 (M^+ – 3PF_6), ^{1}H NMR (CD_3CN): δ = 8.83 (m, 2H), 8.72 (m, 2H), 8.59–8.47 (m, 8H), 8.18–8.06 (m, 10H), 8.04–7.84 (m, 19H), 7.82–7.68 (m, 15H), 7.50–7.42 (m, 5H), 7.40–7.30 (m, 5H).

ACKNOWLEDGMENTS

This work was supported by the European Community (SUSANA project HPRN-CT-2002-00185), PHILIPS (Contract RWC-061-JR-00084-jr), and the Dutch Polymer Institute.

REFERENCES

1. L. De Cola, F. Barigelletti, V. Balzani, R. Hage, J. G. Haasnoot, J. Reedijk, J. G. Vos. *Chem. Phys. Lett.* **178**, 491 (1991).
2. M. Furue, T. Yoshidzumi, S. Kinoshita, T. Kushida, S. Nozakura, M. Kamachi. *Bull. Chem. Soc. Jpn.* **64**, 1632 (1991).
3. L. De Cola, V. Balzani, F. Barigelletti, L. Flamigni, P. Belser, A. Von Zelewsky, M. Frank, F. Vögtle. *Inorg. Chem.* **32**, 5228 (1993).
4. F. Barigelletti, L. Flamigni, V. Balzani, J. P. Collin, J. P. Sauvage, A. Sour, E. C. Constable, A. Thompson. *Coord. Chem. Rev.* **132**, 209 (1994).
5. J. Lehn. *Supramolecular Chemistry: Concepts and Perspectives*, Wiley-VCH, Weinheim (1995).
6. A. P. deSilva, H. Q. N. Gunaratne, T. Gunnlaugsson, A. J. M. Huxley, C. P. McCoy, J. T. Rademacher, T. E. Rice. *Chem. Rev.* **97**, 1515 (1997).
7. K. Kalyanasundaram and M. Grätzel. *Coord. Chem. Rev.* **177**, 347 (1998).
8. M. A. Baldo, D. F. O'Brien, Y. You, A. Shoustikov, S. Sibley, M. E. Thompson, S. R. Forrest. *Nature* **395**, 151 (1998).
9. V. Cleave, G. Yahioglu, P. Le Barny, R. H. Friend, N. Tessler. *Adv. Mater.* **11**, 285 (1999).
10. F. Barigelletti and L. Flamigni. *Chem. Soc. Rev.* **29**, 1 (2000).
11. C. Joachim, J. K. Gimzewski, A. Aviram. *Nature* **408**, 541 (2000).
12. S. Encinas, L. Flamigni, F. Barigelletti, E. C. Constable, C. E. Housecroft, E. R. Schofield, E. Figgemeier, D. Fenske, M. Neuburger, J. G. Vos, M. Zehnder. *Chem.—Eur. J.* **8**, 137 (2002).
13. J. Andersson, F. Puntoriero, S. Serroni, A. Yartsev, T. Pascher, T. Polivka, S. Campagna, V. Sundstrom. *Chem. Phys. Lett.* **386**, 336 (2004).
14. D. Gust, T. A. Moore, A. L. Moore. *Acc. Chem. Res.* **26**, 198 (1993).
15. T. Pullerits and V. Sundstrom. *Acc. Chem. Res.* **29**, 381 (1996).
16. D. Gust, T. A. Moore, A. L. Moore. *Pure Appl. Chem.* **70**, 2189 (1998).
17. D. Gust, T. A. Moore, A. L. Moore. *Acc. Chem. Res.* **34**, 40 (2001).
18. J. F. Nierengarten, N. Armaroli, G. Accorsi, Y. Rio, J. F. Eckert. *Chem.—Eur. J.* **9**, 37 (2003).

19. C. N. Fleming, K. A. Maxwell, J. M. DeSimone, T. J. Meyer, J. M. Papanikolas. *J. Am. Chem. Soc.* **123**, 10336 (2001).
20. A. Juris, L. Prodi, A. Harriman, R. Ziessel, M. Hissler, A. El-Ghayoury, F. Y. Wu, E. C. Riesgo, R. P. Thummel. *Inorg. Chem.* **39**, 3590 (2000).
21. M. Furue, M. Ishibashi, A. Satoh, T. Oguni, K. Maruyama, K. Sumi, M. Kamachi. *Coord. Chem. Rev.* **208**, 103 (2000).
22. A. K. Bilakhiya, B. Tyagi, P. Paul, P. Natarajan. *Inorg. Chem.* **41**, 3830 (2002).
23. A. Borje, O. Kothe, A. Juris. *J. Chem. Soc., Dalton Trans.* 843 (2002).
24. C. Chiorboli, M. A. J. Rodgers, F. Scandola. *J. Am. Chem. Soc.* **125**, 483 (2003).
25. F. Lafolet, J. Chauvin, M. Collomb, A. Deronzier, H. Laguitton-Pasquier, J. C. Lepretre, J. C. Vial, B. Brasme. *Phys. Chem. Chem. Phys.* **5**, 2520 (2003).
26. F. Weldon, L. Hammarstrom, E. Mukhtar, R. Hage, E. Gunneweg, J. G. Haasnoot, J. Reedijk, W. R. Browne, A. L. Guckian, J. G. Vos. *Inorg. Chem.* **43**, 4471 (2004).
27. R. Ziessel, M. Hissler, A. El-Ghayoury, A. Harriman. *Coord. Chem. Rev.* **180**, 1251 (1998).
28. L. De Cola and P. Belser. "Photonic wires containing metal complexes", in *Electron Transfer in Chemistry*, Vol. V, V. Balzani (Ed.), p. 97, Wiley-VCH, Weinheim (2001).
29. F. Scandola, C. Chiorboli, M. T. Indelli, M. A. Rampi. "Covalently linked systems containing metal complexes", in *Electron Transfer in Chemistry*, Vol. III, V. Balzani (Ed.), p. 337, Wiley-VCH, Weinheim (2001).
30. S. Campagna, C. Di Pietro, F. Loiseau, B. Maubert, N. McClenaghan, R. Passalacqua, F. Puntoriero, V. Ricevuto, S. Serroni. *Coord. Chem. Rev.* **229**, 67 (2002).
31. L. De Cola and P. Belser. *Coord. Chem. Rev.* **177**, 301 (1998).
32. F. Scandola, C. A. Bignozzi, C. Chiorboli, M. T. Indelli, M. A. Rampi. *Coord. Chem. Rev.* **97**, 299 (1990).
33. J.-P. Launay. *Chem. Soc. Rev.* **30**, 386 (2001).
34. K. Kalyanasundaram. *Photochemistry of Polypyridine and Porphyrin Complexes*, Academic Press, London (1992).
35. A. Juris, V. Balzani, F. Barigelletti, S. Campagna, P. Belser, A. Von Zelewsky. *Coord. Chem. Rev.* **84**, 85 (1988).
36. V. Balzani, A. Juris, M. Venturi, S. Campagna, S. Serroni. *Chem. Rev.* **96**, 759 (1996).
37. W. B. Davis, W. A. Svec, M. A. Ratner, M. R. Wasielewski. *Nature* **396**, 60 (1998).
38. L. Pascal, J. J. Vanden Eynde, Y. Van Haverbeke, P. Dubois, A. Michel, U. Rant, E. Zojer, G. Leising, L. O. Van Dorn, N. E. Gruhn, J. Brédas, J. L. Cornil. *J. Phys. Chem. B* **106**, 6442 (2002).
39. S. Welter, N. Salluce, P. Belser, L. De Cola. *Coord. Chem. Rev.* (2005). Available on the Web.
40. T. Tzalis. *J. Am. Chem. Soc.* **119**, 852 (1997).
41. E. Baranoff, I. M. Dixon, J.-P. Collin, J.-P. Sauvage, B. Ventura, L. Flamigni. *Inorg. Chem.* **43**, 3057 (2004).
42. S. Chodorowski-Kimmes, M. Beley, J.-P. Collin, J.-P. Sauvage. *Tetrahedron Lett.* **37**, 2963 (1996).
43. S. Serroni, S. Campagna, F. Puntoriero, C. Di Pietro, N. D. McClenaghan, F. Loiseau. *Chem. Soc. Rev.* **30**, 367 (2001).
44. N. Miyaura and A. Suzuki. *Chem. Rev.* **95**, 2457 (1995).
45. A. Suzuki. *J. Organomet. Chem.* **576**, 147 (1999).
46. S. Welter, A. Bennetti, N. Rot, N. Salluce, P. Belser, A. C. Grimsdale, K. Müllen, M. Lutz, A. L. Spek, L. De Cola. *Inorg Chem.* (2005). In press.
47. M. Fukuda, K. Sawada, K. Yoshino. *J. Polym. Sci., Polym. Chem.* **31**, 2465 (1993).
48. B. Schlicke, P. Belser, L. De Cola, E. Sabbioni, V. Balzani. *J. Am. Chem. Soc.* **121**, 4207 (1999).
49. D. L. Dexter. *J. Chem. Phys.* **21**, 836 (1953).
50. G. L. Closs and J. R. Miller. *Science* **240**, 440 (1988).
51. J. N. Onuchic and D. N. Beratan. *J. Am. Chem. Soc.* **109**, 6771 (1987).

52. R. J. Cave, D. V. Baxter, W. A. Goddard, J. D. Baldeshwieler. *J. Chem. Phys.* **87**, 926 (1987).
53. V. Balzani and F. Scandola. *Supramolecular Photochemistry*, Horwood, Chichester, UK (1991).
54. P. Coppo, M. Duati, V. Kozhevnikov, J. W. Hofstraat, L. De Cola. *Angew. Chem., Int. Ed.* **44**, 1806 (2005).
55. O. Bossart, L. De Cola, S. Welter, J. Calzaferri. *Chem.—Eur. J.* **10**, 5771 (2004).